Int. J. Solids Structures Vol. 30, No. 21, pp. 2895–2909, 1993
Printed in Great Britain

0020–7683/93 $6.00+ .00

NONLINEAR DYNAMIC BUCKLING OF DISCRETE STRUCTURAL SYSTEMS UNDER IMPACT LOADING

ANTHONY N. KOUNADIS
National Technical University of Athens, 42 Patission St., Athens 106 82, Greece

(*Received* 5 *January* 1993)

Abstract—Nonlinear dynamic buckling of discrete dissipative or nondissipative, nonlinearly elastic, structural systems, geometrically perfect or imperfect, under impact loading is thoroughly examined. Applying the law of impulse momentum one can determine analytically the initial conditions valid immediately after impact. Thereafter, the response of the system is governed by a set of autonomous highly nonlinear ordinary differential equations. Using an efficient and qualitative analysis exact and lower–upper bound dynamic buckling estimates, very useful for structural design purposes, are established without integrating the aforementioned nonlinear initial-value problem. The analysis is supplemented by a variety of numerical results of a two-degrees-of-freedom dissipative model. From these results it is clearly shown how the point attractor response of the system is changed after a sudden jump to dynamic buckling occurring through a global dynamic bifurcation.

1. INTRODUCTION

Dynamic buckling of dissipative or nondissipative discrete systems under step constant directional (conservative) loading of infinite, finite or very short duration as well as pertinent criteria for establishing exact and lower–upper bound buckling estimates have been critically presented in several recent studies by the author and his associates (Raftoyiannis and Kounadis, 1988; Kounadis *et al.*, 1990; Kounadis and Raftoyiannis, 1990; Kounadis, 1991a, 1993). Dynamic buckling is associated with a finite jump and then with an escaped motion occurring through an unstable equilibrium point (dissipative system) or a non-equilibrium point lying in the vicinity of an unstable equilibrium path (non-dissipative system). Hence dynamic buckling takes place via a global bifurcation which cannot be established unless a nonlinear dynamic analysis is employed. Recall that as dynamic bifurcation is defined a sudden qualitative change of the system response occurs at a certain value of a smoothly varying control parameter. The case of dynamic buckling for statically stable systems which also exhibit a complementary (physically unacceptable) path is also studied in detail (Kounadis, 1991b; Kalathas and Kounadis, 1991).

The objective of this work is to extend the previous studies to the case of dynamic buckling under impact loading. This is achieved by using the law of impulse momentum together with several main concepts of the theory of dynamical systems in a comprehensive but mathematically rigorous way. The response of the system after impact is described by a system of highly nonlinear autonomous ordinary differential equations. The analysis is applied to a two-degrees-of-freedom dissipative model but it can be easily extended to structural systems with more than two degrees of freedom.

Without solving the highly nonlinear system of ordinary differential equations exact as well as lower–upper bound buckling estimates are readily established using a comprehensive qualitative analysis. The accuracy of these estimates is checked through numerical solution based on the fourth order numerical scheme of Runge–Kutta. On the other hand the accuracy of the numerical integration in the case of large time solutions is conveniently checked with the aid of the total energy equation.

2. GENERAL CONSIDERATIONS

Consider a general initially imperfect n-mass structural system under impact loading. It is assumed that immediately after impact the large dynamic response of the system is described by the nonlinear autonomous ordinary differential equations (ODE) of Lagrange.

These equations in terms of generalized displacements q_i and generalized velocities $\dot{q}_i$ $(i = 1, \ldots, n)$ are given as

$$\frac{d}{dt}\left(\frac{\partial K}{\partial \dot{q}_i}\right) - \frac{\partial K}{\partial q_i} + \frac{\partial V_T}{\partial q_i} + \frac{\partial F}{\partial \dot{q}_i} = 0 \quad (i = 1, \ldots, n), \tag{1}$$

where the dots denote differentiation with respect to time t; $K = (1/2)\dot{q}^T[\alpha_{ij}]\dot{q}$ is the positive definite function of the total kinetic energy with nondiagonal elements $\alpha_{ij} = \alpha_{ij}(q_1, \ldots, q_n)$ and $\dot{q}^T$, being the transpose of the vector $\dot{q}$ with components $\dot{q}_i$ $(i = 1, \ldots, n)$; $V_T = V_T(q_1, \ldots, q_n; \lambda)$ is the total potential energy which is assumed to be a linear function of the loading parameter λ resulting after impact; $F = (1/2)\dot{q}^T[c_{ij}]\dot{q}$ is the non-negative definite (viscous) dissipation function of Rayleigh with coefficients c_{ij} which might be functions of q_i [i.e. $c_{ij} = c_{ij}(q_1, \ldots, q_n)$]. The loading λ is considered as the main control parameter for the occurrence of static and dynamic bifurcation, as it was defined in Section 1. It is also assumed that this system under the same loading, λ, applied statically exhibits a limit point instability.

A crucial point for the subsequent dynamic analysis is the determination of the initial conditions. Regarding the initial displacements of the above geometrically imperfect system one can write

$$q_i(t = 0) = q_i^0, \quad (i = 1, \ldots, n). \tag{2}$$

However, the establishment of the initial velocities

$$v_i = \dot{q}_i(t = 0) = \dot{q}_i^0, \quad (i = 1, \ldots, n) \tag{3}$$

is not a very easy task. This can be achieved by employing (for the state immediately after impact) the law of impulse momentum together with the vectorial kinematic relations among the velocities of the masses. Then one can determine the initial velocities $\dot{\mathbf{q}}_i^0$ as functions of the impact loading. If K^0 is the corresponding initial kinetic energy one can write the total energy E, valid at any time $t > 0$, as follows:

$$E = K + V_T + 2\int_0^t F\,dt' = K^0, \tag{4}$$

where $K^0 = (1/2)v^T[\alpha_{ij}]v$ and $v = v(v_1, \ldots, v_n)$ with $v_i = q_i^0$. Equation (4) is also used for checking the accuracy of large time solutions due to accumulation of error.

For the sake of simplicity the above analysis will be illustrated by using the two-degrees-of-freedom dissipative model of Ziegler. However, it can be easily extended to multi-degrees-of-freedom systems.

Ziegler's model

Ziegler's two-degrees-of-freedom cantilevered model shown in Fig. 1 consists of two rigid weightless links of equal length l, interconnected with each other and being supported by frictionless hinges and corresponding nonlinearly elastic rotational springs of quadratic type. The two springs are also associated with corresponding linear viscous dampers. Two concentrated masses m_1 and m_2 are placed at B and C. The unstressed configuration (before impact) is specified by the initial displacements $\mathbf{q}_i^0 = q_i^0(q_{iH}^0, q_{iV}^0)$, where q_{iH}^0 and q_{iV}^0 $(i = 1, 2)$ are the horizontal and vertical components given by

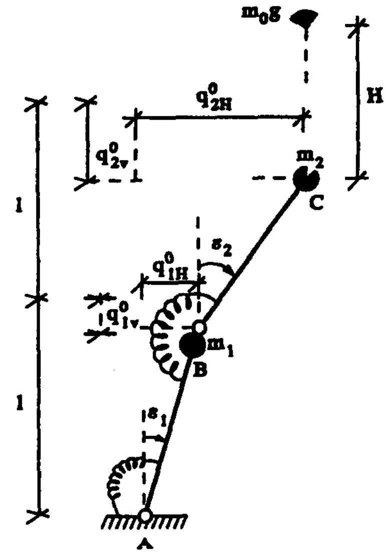

Fig. 1. Ziegler's geometrically imperfect model under impact load.

$$\left.\begin{aligned} q^0_{1H} &= l\sin\varepsilon_1, & q^0_{2H} &= l(\sin\varepsilon_1+\sin\varepsilon_2) \\ q^0_{1V} &= l(1-\cos\varepsilon_1) & q^0_{2V} &= l(2-\cos\varepsilon_1-\cos\varepsilon_2) \end{aligned}\right\}, \tag{5}$$

where ε_1 and ε_2 are the initial geometric imperfections with the sign convention for the angles of rotation shown in Fig. 1.

A body of weight m_0g (g is the gravitational acceleration) falling from a height H strikes centrally the tip mass m_2 with initial velocity $v_0 = \sqrt{2gH}$. A completely plastic impact is postulated (i.e. the coefficient of restitution is zero); thus both the striking body and the tip mass attain immediately after impact the same velocity $\mathbf{v}_2$ $(\dot{\mathbf{q}}^0_2)$ and do not separate thereafter (Goldsmith, 1960). At the same time, the mass m_1 assumes a velocity $\mathbf{v}_1$ $(=\dot{\mathbf{q}}^0_1)$ normal to the link AB. The direction and magnitude of $\mathbf{v}_2$ and the magnitude of $\mathbf{v}_1$ are to be determined. It is assumed that the response of the model after impact remains elastic throughout deformation. It is convenient now to consider two characteristic configuration stages (Fig. 2).

Stage I refers to the state immediately after impact (with masses m_1 and $M = m_0+m_2$) which corresponds to the initial conditions specified by the initial ($t = 0$) displacements $\mathbf{q}^0_i$ ($i = 1, 2$) and velocities $\mathbf{v}_i = \dot{\mathbf{q}}^0_i$ ($i = 1, 2$), where the components of $\mathbf{q}^0_i(q^0_{iH}, q^0_{iV})$ are given in eqns (5). $\mathbf{R}$ is the reacting force at the support A in the direction AB assuming that both springs are unstressed at $t = 0$.

Stage II corresponds to the deformed configuration state after impact ($t > 0$) and under the influence of the vertical loading m_0g. This stage is defined by the displacements and velocities vectors $\mathbf{q}_i = \mathbf{q}^0_i(q_{iH}, q_{iV})$ and $\dot{\mathbf{q}}_i = \dot{\mathbf{q}}_i(\dot{q}_{iH}, \dot{q}_{iV})$, whose components are given by

$$\left.\begin{aligned} q_{1H} &= l(\sin\vartheta_1-\sin\varepsilon_1), & q_{2H} &= l(\sin\vartheta_1+\sin\vartheta_2-\sin\varepsilon_1-\sin\varepsilon_2) \\ q_{1V} &= l(\cos\varepsilon_1-\cos\vartheta_1), & q_{2V} &= l(\cos\varepsilon_1+\cos\varepsilon_2-\cos\vartheta_1-\cos\vartheta_2) \end{aligned}\right\}, \tag{6}$$

$$\left.\begin{aligned} \dot{q}_{1H} &= l\dot{\vartheta}_1\cos\vartheta_1, & \dot{q}_{2H} &= l(\dot{\vartheta}_1\cos\vartheta_1+\dot{\vartheta}_2\cos\vartheta_2) \\ \dot{q}_{1V} &= l\dot{\vartheta}_1\sin\vartheta_1, & \dot{q}_{2V} &= l(\dot{\vartheta}_1\sin\vartheta_1+\dot{\vartheta}_2\sin\vartheta_2) \end{aligned}\right\}. \tag{7}$$

With the aid of relations (6) and (7) the magnitudes of the component vectors $\mathbf{q}_i$ and $\dot{\mathbf{q}}_i$ ($i = 1, 2$) at $t > 0$ are

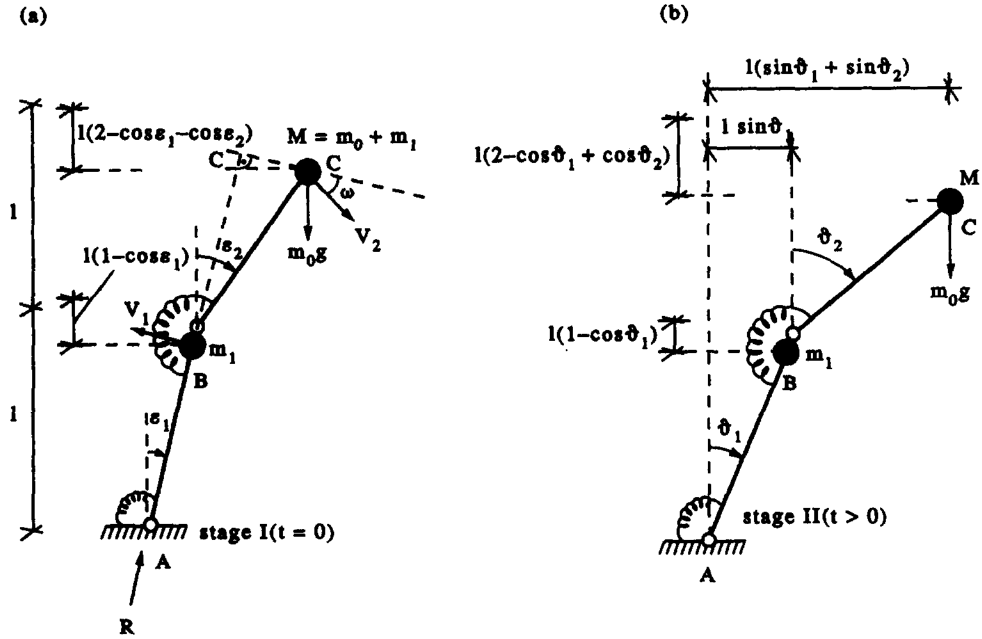

Fig. 2. Initial (unstressed) and deformed configuration, at $t = 0$ (stage I) and $t > 0$ (stage II).

$$
\begin{aligned}
q_1 &= \sqrt{q_{1H}^2+q_{1V}^2} = l\sqrt{(\sin\vartheta_1-\sin\varepsilon_1)^2+(\cos\varepsilon_1-\cos\vartheta_1)^2},\\
q_2 &= \sqrt{q_{2H}^2+q_{2V}^2} = l\sqrt{(\sin\vartheta_1+\sin\vartheta_2-\sin\varepsilon_1-\sin\varepsilon_2)^2+(\cos\varepsilon_1+\cos\varepsilon_2-\cos\vartheta_1-\cos\vartheta_2)^2},\\
\dot q_1 &= \sqrt{\dot q_{1H}^2+\dot q_{1V}^2} = l\dot\vartheta_1,\\
\dot q_2 &= \sqrt{\dot q_{2H}^2+\dot q_{2V}^2} = l\sqrt{\dot\vartheta_1^2+\dot\vartheta_2^2+2\dot\vartheta_1\dot\vartheta_2\cos(\vartheta_1-\vartheta_2)}.
\end{aligned} \tag{8}
$$

The kinetic energy K, the potential energy U_T, and the Rayleigh dissipation function F are

$$
\begin{aligned}
\frac{K}{ML^2} &= \frac{1}{2}\left(\frac{m_1}{M}\right)\dot\vartheta_1^2+\tfrac{1}{2}[\dot\vartheta_1^2+\dot\vartheta_2^2+2\dot\vartheta_1\dot\vartheta_2\cos(\vartheta_1-\vartheta_2)],\\
V_T &= \frac{U_T}{k} = \tfrac{1}{2}(\vartheta_1-\varepsilon_1)^2+\tfrac{1}{3}\delta_1(\vartheta_1-\varepsilon_1)^3+\tfrac{1}{2}(\vartheta_2-\varepsilon_2-\vartheta_1+\varepsilon_1)^2\\
&\quad +\tfrac{1}{3}\delta_2(\vartheta_2-\varepsilon_2-\vartheta_1+\varepsilon_1)^3-\lambda(\cos\varepsilon_1-\cos\vartheta_1+\cos\varepsilon_2-\cos\vartheta_2)\quad\text{with}\quad \lambda=\frac{m_0gl}{k},\\
F &= \tfrac{1}{2}c_1\dot\vartheta_1^2+\tfrac{1}{2}c_2(\dot\vartheta_2-\dot\vartheta_1)^2,
\end{aligned} \tag{9}
$$

where k is the linear spring component common for both springs and δ_i $(i = 1, 2)$ are the nonlinear components of the corresponding quadratic springs. If $\delta_i > 0$ (<0) the corresponding spring is of hard (soft) type.

3. DETERMINATION OF INITIAL CONDITIONS

Immediately after plastic impact (i.e. at $t = 0$) application of the law of impulse momentum yields the following equation in vectorial form [see Fig. 2(a, b)]:

$$\left.\begin{array}{l} m_0\mathbf{v}_0+\mathbf{R}\Delta t = M\mathbf{v}_2+m_1\mathbf{v}_1 \\ \text{where} \quad \mathbf{v}_1 = \dot{\mathbf{q}}_1^0 \quad \text{and} \quad \mathbf{v}_2 = \dot{\mathbf{q}}_2^0 \end{array}\right\}. \tag{10}$$

The projections of eqn (10) in the direction AB and its normal are, respectively,

$$\left.\begin{array}{l} m_0 v_0 \cos\varepsilon_1 - R\Delta t = Mv_2 \sin\omega \\ m_0 v_0 \sin\varepsilon_1 = Mv_2\cos\omega - m_1 v_1 \end{array}\right\}, \tag{11}$$

where $R\Delta t$ and the angle ω are determined as follows.

Applying the law of the impulse momentum on the mass m_1 at the joint B in the direction $B'B$ (normal to the direction BC) we get (see Fig. 3)

$$R\Delta t = m_1 v_1 \cot(\varepsilon_2-\varepsilon_1). \tag{12}$$

On the other hand taking into account that the initial angular velocitiy of the link BC is $\dot{\vartheta}_2(0)$ one can write the following relation between the velocity vectors $\mathbf{v}_2$ and $\mathbf{v}_1$:

$$\mathbf{v}_2 = \mathbf{v}_1 + l\dot{\vartheta}_2(0). \tag{13}$$

The projections of this equation in the direction AB and the direction of its normal are

$$\left.\begin{array}{l} v_2\sin\omega = l\dot{\vartheta}_2(0)\sin(\varepsilon_2-\varepsilon_1) \\ v_2\cos\omega = l\dot{\vartheta}_2(0)\cos(\varepsilon_2-\varepsilon_1)-v_1 \end{array}\right\}. \tag{14}$$

Given that

$$v_1 = -l\dot{\vartheta}_1(0), \tag{15}$$

eqns (14) yield

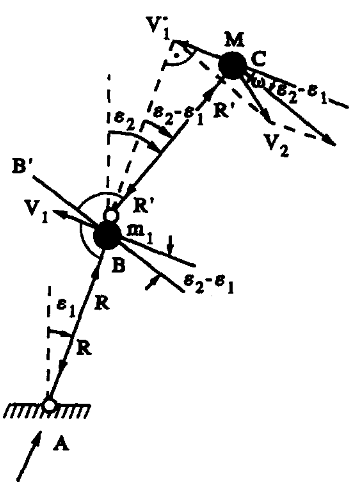

Fig. 3. Internal forces and kinematics of the velocity vectors at $t = 0$.

$$\left.\begin{aligned} \tan\omega &= \frac{\dot{\vartheta}_2(0)\sin(\varepsilon_2-\varepsilon_1)}{\dot{\vartheta}_1(0)+\dot{\vartheta}_2(0)\cos(\varepsilon_2-\varepsilon_1)} \\ v_2 &= l\sqrt{\dot{\vartheta}_1^2(0)+\dot{\vartheta}_2^2(0)+2\dot{\vartheta}_1(0)\dot{\vartheta}_2(0)\cos(\varepsilon_2-\varepsilon_1)} \end{aligned}\right\}. \tag{16}$$

On the other hand, eqns (11) by virtue of relations (12) and (15) give

$$\left.\begin{aligned} \tan\omega &= \frac{m_0v_0\cos\varepsilon_1+m_1l\dot{\vartheta}_1(0)\cot(\varepsilon_2-\varepsilon_1)}{m_0v_0\sin\varepsilon_1-m_1l\dot{\vartheta}_1(0)} \\ v_2 &= \frac{\sqrt{1+\tan^2\omega}}{M}[m_0v_0\sin\varepsilon_1-m_1l\dot{\vartheta}_1(0)] \end{aligned}\right\}. \tag{17}$$

Substituting the last expressions of $\tan\omega$ and v_2 into the corresponding eqns (16), after elaboration, we get

$$\frac{m_1l}{m_0v_0}\left[\cos(\varepsilon_2-\varepsilon_1)-\left(\frac{M+m_1}{M}\right)\frac{1}{\cos(\varepsilon_2-\varepsilon_1)}\right]\dot{\vartheta}_1^2(0)+\left[\cos\varepsilon_1\sin(\varepsilon_2-\varepsilon_1)\right.$$

$$\left.-\left(\frac{M+m_1}{M}\right)\cos\varepsilon_2\tan(\varepsilon_2-\varepsilon_1)+\left(\frac{m_1}{M}\right)\frac{\sin\varepsilon_1}{\cos(\varepsilon_2-\varepsilon_1)}\right]\dot{\vartheta}_1(0)$$

$$+\frac{m_0v_0}{Ml}\sin\varepsilon_1\cos\varepsilon_2\tan(\varepsilon_2-\varepsilon_1)=0,$$

$$\dot{\vartheta}_2(0)=\frac{1}{\cos(\varepsilon_2-\varepsilon_1)}\left[\frac{m_0v_0}{Ml}\sin\varepsilon_1-\left(\frac{M+m_1}{M}\right)\dot{\vartheta}_1(0)\right]. \tag{18}$$

From eqns (18) we can determine $\dot{\vartheta}_1(0)$ and $\dot{\vartheta}_2(0)$ in terms of known quantities.

4. GOVERNING EQUATIONS

Introducing the dimensionless quantities

$$\left.\begin{aligned} &\tau=t\sqrt{k/Ml^2},\quad \Theta(\tau)=\vartheta(t),\quad \mu_1=m_1/M,\quad \mu_0=m_0/M \\ &\bar{v}_0=v_0\sqrt{M/k},\quad \bar{c}_i=\frac{c_i}{l\sqrt{kM}} \end{aligned}\right\}, \tag{19}$$

eqns (1) by virtue of relations (9) give

$$\left.\begin{aligned} (1+\mu_1)\ddot{\Theta}_1+\ddot{\Theta}_2\cos(\Theta_1-\Theta_2)+\dot{\Theta}_2^2\sin(\Theta_1-\Theta_2)+(\bar{c}_1+\bar{c}_2)\cdot\dot{\Theta}_1-\bar{c}_2\dot{\Theta}_2+\frac{\partial V_T}{\partial\Theta_1}=0 \\ \ddot{\Theta}_2+\ddot{\Theta}_1\cos(\Theta_1-\Theta_2)-\dot{\Theta}_1^2\sin(\Theta_1-\Theta_2)+\bar{c}_2\dot{\Theta}_2-\bar{c}_2\dot{\Theta}_1+\frac{\partial V_T}{\partial\Theta_2}=0 \end{aligned}\right\}, \tag{20}$$

where

$$\left.\begin{aligned}\frac{\partial V_T}{\partial \Theta_1} &= 2(\Theta_1-\varepsilon_1)-(\Theta_2-\varepsilon_2)+\delta_1(\Theta_1-\varepsilon_1)^2-\delta_2(\Theta_1-\varepsilon_1-\Theta_2+\varepsilon_2)^2-\lambda\sin\Theta_1\\ \frac{\partial V_T}{\partial \Theta_2} &= -(\Theta_1-\varepsilon_1)+\Theta_2-\varepsilon_2+\delta_2(\Theta_1-\varepsilon_1-\Theta_2+\varepsilon_2)^2-\lambda\sin\Theta_2\end{aligned}\right\}. \tag{21}$$

Note that the loading $\lambda = m_0 gl/k$ is acting (for $t > 0$) as step load of infinite duration.

The associated initial conditions (18) due to relations (19) become

$$\frac{\mu_1}{\mu_0\bar{v}_0}[\mu_1+\sin^2(\varepsilon_2-\varepsilon_1)]\dot{\Theta}_1^2(0)-[\cos\varepsilon_2\cos(\varepsilon_1-\varepsilon_1)\cdot\sin(\varepsilon_2-\varepsilon_1)$$
$$-(1+\mu_1)\cos\varepsilon_2\sin(\varepsilon_2-\varepsilon_1)+\mu_1\sin\varepsilon_1]\dot{\Theta}_1(0)$$
$$-\mu_0\bar{v}_0\sin\varepsilon_1\cos\varepsilon_2\sin(\varepsilon_2-\varepsilon_1)=0,$$

$$\dot{\Theta}_2(0)=\frac{1}{\cos(\varepsilon_2-\varepsilon_1)}[\mu_0\bar{v}_0\sin\varepsilon_1-(1+\mu_1)\dot{\Theta}_1(0)]. \tag{22}$$

Equations (20) and (22) define completely the nonlinear initial-value problem under discussion. In the case where $\varepsilon_1 = \varepsilon_2 = \varepsilon \neq 0$ the initial conditions (22) become

$$\dot{\Theta}_1(0)=\frac{\mu_0\bar{v}_0}{\mu_1}\sin\varepsilon,\quad \dot{\Theta}_2(0)=-\dot{\Theta}_1(0). \tag{23a}$$

If $\varepsilon_1 = \varepsilon_2 = 0$ (perfect system) eqns (22) give

$$\dot{\Theta}_1(0)=\dot{\Theta}_2(0)=0. \tag{23b}$$

Note also that setting $\bar{v}_0 = 0$ in eqns (22) we obtain the case of a geometrically imperfect model under a step load of infinite duration with initial conditions $\Theta_1(0) = \varepsilon_1$, $\Theta_2(0) = \varepsilon_2$, $\dot{\Theta}_1(0) = \dot{\Theta}_2(0) = 0$.

The total energy E in dimensionless form by means of relations (4), (9) and (19) becomes

$$E = K+V_T+2\int_0^\tau F\,d\tau' = K^0, \tag{24}$$

where $K = K/k$; V_T is given in relation (9), while

$$\left.\begin{aligned}F &= F/k = \tfrac{1}{2}[\bar{c}_1\dot{\Theta}_1^2+\bar{c}_2(\dot{\Theta}_1-\dot{\Theta}_2)^2]\\ K^0 &= \tfrac{1}{2}[(1+\mu_1)\dot{\Theta}_1^2(0)+\dot{\Theta}_2^2(0)+2\dot{\Theta}_1(0)\dot{\Theta}_2(0)\cos(\varepsilon_2-\varepsilon_1)]\end{aligned}\right\}. \tag{25}$$

5. QUALITATIVE ANALYSIS

With the aid of the development that follows one can establish the exact dynamic buckling load for the case of vanishing but non-zero damping without solving the nonlinear initial-value problem of eqns (20) and (22). To this end a brief explanation of the mechanism of dynamic buckling will be given below.

As is known the above system under step loading of infinite duration exhibits a point attractor response (Kounadis, 1991a). The precritical (prior to limit point) equilibrium states which are asymptotically stable (associated with complex conjugate Jacobian eigenvalues having negative real parts) capture the motion which for $t \to \infty$ converges towards the corresponding (stable) equilibrium point. This can be readily understood with the aid of a two-degrees-of-freedom system shown in Fig. 4. From Fig. 4 it is also clear that the unstable equilibrium points of the postbuckling path are saddle points which in one (or more) direction act as repellors, while in the remaining directions, as attractors. As is known at a saddle point at least one pair of the Jacobian eigenvalues has a positive real part which implies a divergent motion.

Each stable equilibrium point has its own basin of attraction; any motion originating in it, leads after the decay of transients (as $t \to \infty$) to the corresponding stable equilibrium point. Each saddle point is associated with invariant smooth inset (stable) and outset (unstable) manifolds asymptotic to it. The inset manifold acts as attractor capturing the motion, while the outset manifold acts as repellor sending away the motion (escaped motion). The inset manifold is identified as the set of trajectories asymptotic to a saddle as $t \to \infty$ (attractor), while the outset is the set of trajectories asymptotic to a saddle as $t \to -\infty$ (repellor). The inset and outset smooth manifolds are approximated by straight lines in two dimensions (see Fig. 4), whereas in higher dimensions they may be curves, smooth surface or hypersurfaces.

Consider at each level of the loading λ the basin of attraction of the corresponding stable equilibrium point as well as the invariant inset and outset manifolds of the corresponding (to the same loading) saddle point. As the loading increases from zero at a certain value of the loading λ there exists a stable equilibrium point with a basin of attraction whose boundary touches the inset and outset manifolds of the corresponding (to the same loading) saddle point. Then the motion, after several oscillations, is captured by the inset (stable) manifold and when it reaches the saddle point escapes through the outset (unstable) manifold. Hence, the saddle point is the threshold via which an escaped motion takes place. Such escaped motion is associated either with an "unbounded" motion or usually with a jump to another farther stable equilibrium position capturing the motion for $t \to \infty$ (attractor). In either case we consider that the above escaped motion leads to dynamic buckling. Thus, dynamic buckling is defined, in a more general sense, as that state for which an infinitesimal variation of the loading produces a large displacement response. The corresponding (to that state) minimum loading is defined as the dynamic buckling load λ_{DD} which has as upper bound the limit point load λ_s (Kounadis, 1991a); that is $\lambda_{DD} < \lambda_s$.

On the other hand from the expression of the total energy [eqn (4) or eqn (24)] it is clear that throughout the motion (including the state of dynamic buckling) the varying quantity $V_T - K^0$ is negative definite. Given that dynamic buckling takes place via a saddle point, corresponding to $\lambda_{DD} < \lambda_s$ the kinetic energy at that instant becomes zero. Then eqn (24) yields

$$V_T = -2\int_0^\tau F\,d\tau' + K^0. \tag{26}$$

Since $\lambda_{DD} < \lambda_s$ the last condition is valid provided that

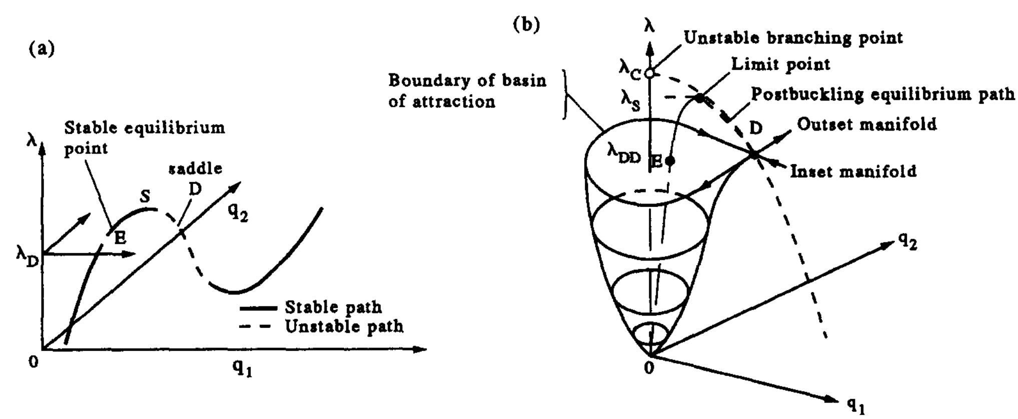

Fig. 4. Stable equilibrium point E with its basin of attraction and saddle point D with its inset and outset manifolds for a two-degrees-of-freedom system.

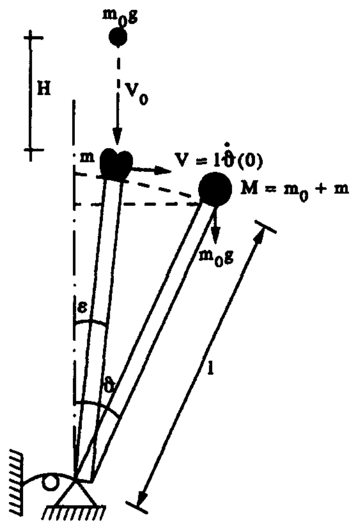

Fig. 5. Single-degree-of-freedom model under impact loading.

$$V_T(\Theta_i^s;\lambda_s) \leqslant K^0 - 2\int_0^\tau F\,d\tau \quad (i = 1, 2, \ldots), \tag{27}$$

where Θ_i^s are the angles of rotation at the limit point.

Equation (26) for vanishing (nonzero) damping ($c_1, c_2 \to 0$) implies

$$V_T = +K^0, \tag{26a}$$

where K^0 is evaluated by means of relations (25) and (22). Condition (26a) along with the equilibrium equations

$$\frac{\partial V_T}{\partial \Theta_1} = \frac{\partial V_T}{\partial \Theta_2} = 0 \tag{28}$$

yield the exact dynamic buckling load $\tilde{\lambda}_D$ for vanishing (but nonzero) damping without integrating the nonlinear initial-value problem of eqns (20) and (22). In the case of a nonzero damping if the amount of damping decreases $\tilde{\lambda}_D$ approaches the accurate dynamic buckling load λ_{DD}. For vanishing but nonzero damping eqns (26a) and (28) yield

$$\tilde{\lambda}_D \to \lambda_{DD}. \tag{29}$$

Hence $\tilde{\lambda}_D$ is also a lower bound estimate of the exact dynamic buckling load λ_{DD}. In conclusion,

$$\tilde{\lambda}_D < \lambda_{DD} < \lambda_s. \tag{30}$$

This finding was also presented by Kounadis (1991a) using a slightly different procedure.

While the precise modelling of a dynamical system should always include damping, one could consider the unrealistic case of zero damping. In this case, according to the (sufficient) inflection point criterion for dynamic buckling (Kounadis, 1991a) the point through which an escaped motion occurs is a nonequilibrium point which lies in the vicinity of the unstable postbuckling equilibrium path. This implies that the kinetic energy K is not zero at the instant of dynamic buckling. Denoting by λ_D the dynamic buckling load of the undamped system it can be established using the procedure outlined by Kounadis (1991a) that $\tilde{\lambda}_D$ is less than λ_D. Then, inequality (30) becomes

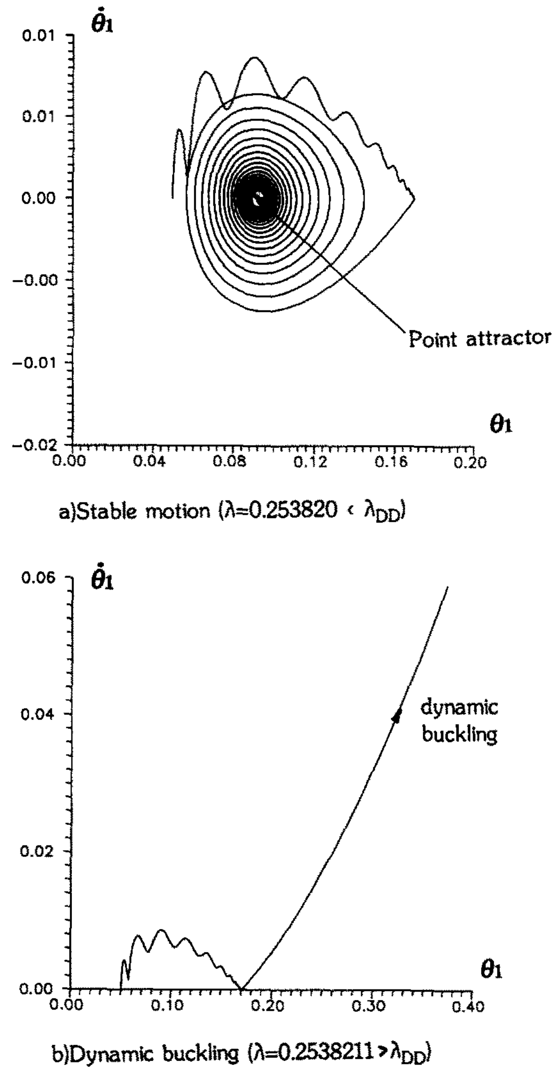

Fig. 6. Phase plane portraits for the case of step loading of infinite duration with $\delta_1 = -2.5$, $\delta_2 = -0.75$, $\varepsilon_1 = 0.05$, $\varepsilon_2 = 0$, $\bar{c}_1 = 0.04$, $\bar{c}_2 = 0.06$, $\mu_1 = 1.8$, $\bar{v}_0 = 0$.

$$\tilde{\lambda}_D < \lambda_D < \lambda_{DD} < \lambda_s. \tag{31}$$

Hence $\tilde{\lambda}_D$ obtained through eqns (26a) and (28) is a lower bound dynamic buckling estimate regardless of whether or not damping is included.

This finding should be slightly modified in case of a single-degree-of-freedom model. Consider the initially imperfect model under impact loading shown in Fig. 5. The Lagrange equation of motion (Kounadis and Raftoyiannis, 1990) and the corresponding initial conditions are

$$\left.\begin{array}{c}\ddot{\Theta}+(\Theta-\varepsilon)[1+\delta(\Theta-\varepsilon)]+\bar{c}\dot{\Theta}-\lambda\sin\Theta=0\\ \Theta(0)=\varepsilon,\quad \dot{\Theta}(0)=\mu_0\bar{v}_0\sin\varepsilon\end{array}\right\}. \tag{32}$$

For $\bar{v}_0 = 0$ the impact load reduces to a step load of infinite duration. Note also that numerical integration of eqns (32) for the case of a geometrically perfect model ($\varepsilon = 0$) under impact load is possible only by assuming a negligibly small (but nonzero) value of ε.

For an undamped single-degree-of-freedom model the inflection point (sufficient) criterion for dynamic buckling yields that an escaped motion takes place via a saddle (i.e.

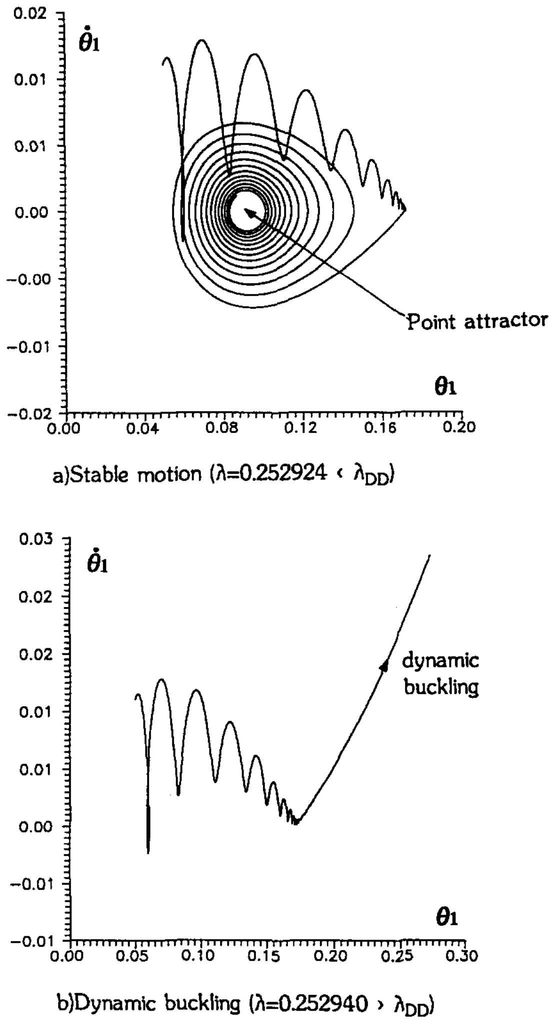

Fig. 7. Phase plane portraits for the case of impact loading with $\delta_1 = -2.5$, $\delta_2 = -0.75$, $\varepsilon_1 = 0.05$, $\varepsilon_2 = 0$, $\bar{c}_1 = 0.04$, $\bar{c}_2 = 0.06$, $\mu_1 = 1.8$, $\mu_0 = 0.1$, $\bar{v}_0 = 4$.

equilibrium) point on the unstable postbuckling equilibrium path. Then the kinetic energy K and the Rayleigh dissipation functions F are zero and therefore condition (26a) becomes

$$V_T = K^0$$

or

$$\tfrac{1}{2}(\Theta-\varepsilon)^2+\frac{\delta}{3}(\Theta-\varepsilon)^3-\lambda(\cos\varepsilon-\cos\Theta) = \tfrac{1}{2}\mu_0^2\bar{v}_0^2\sin^2\varepsilon. \tag{33}$$

Solving this equation along with the equilibrium equation $\partial V/\partial\Theta = 0$ or

$$\Theta-\varepsilon+\delta(\Theta-\varepsilon)^2-\lambda\sin\Theta = 0 \tag{34}$$

with respect to Θ and λ for given values of μ_0, $\bar{v}_0$, δ and ε we obtain the exact dynamic buckling load for the undamped model under impact load. Namely, for the case of a single-degree-of-freedom model

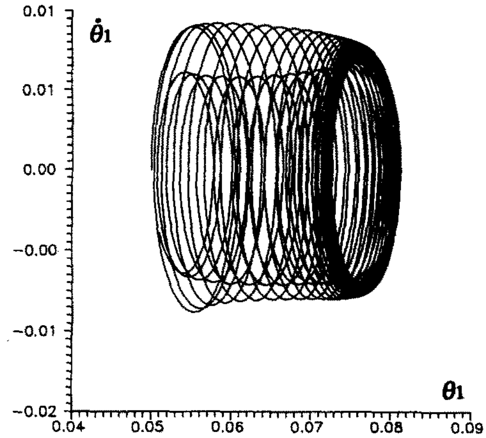

a)Stable motion (λ=0.355247 < λ_{DD})

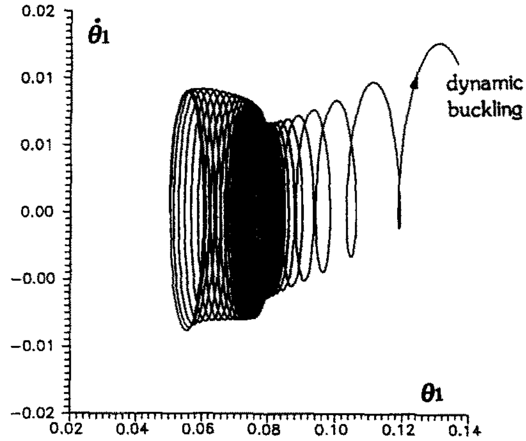

b)Dynamic buckling (λ=0.355248 > λ_{DD})

Fig. 8. Phase plane portraits for the case of step loading of infinite duration with $\delta_1 = -2.5$, $\delta_2 = -0.75$, $\varepsilon_1 = 0.05$, $\varepsilon_2 = -0.031$, $\bar{c}_1 = 0.001$, $\bar{c}_2 = 0.001$, $\mu_1 = 1.84$, $\bar{v}_0 = 0$.

$$\tilde{\lambda}_D \equiv \lambda_D < \lambda_{DD} < \lambda_s. \tag{35}$$

6. NUMERICAL RESULTS AND DISCUSSION

A variety of numerical results associated with corresponding geometric configurations of an imperfect model under impact load ($\bar{v}_0 \neq 0$) as well as under step load of infinite duration are given below.

Consider first a two-degrees-of-freedom model with $\varepsilon_1 = 0.05$, $\varepsilon_2 = 0$, $\delta_1 = -2.5$, $\delta_2 = -0.75$ which loses its static stability via a limit point at a critical load $\lambda_s = 0.267713$. If $\mu_1 = 1.8$ and $\bar{v}_0 = 0$ dynamic buckling under step load of infinite duration occurs at $\lambda_D = 0.252641$ for the undamped model, and at $\lambda_{DD} = 0.253821$ for a damped model with $\bar{c}_1 = 0.04$ and $\bar{c}_2 = 0.06$. The dynamic buckling load for vanishing (but nonzero) damping obtained from eqns (26a) (for $K^0 = 0$) and (28) is equal to $\tilde{\lambda}_D = 0.252277$ namely 1.5% smaller than $\lambda_D = 0.252641$ which corresponds to the undamped model (Kounadis, 1991a). The same model under impact load with $\bar{v}_0 = 4$ and $\mu_0 = 0.1$ buckles dynamically at a load $\lambda_D = 0.251505$ (undamped model) and $\lambda_{DD} = 0.252925$ (damped model with $\bar{c}_1 = 0.04$ and $\bar{c}_2 = 0.06$). The load for vanishing damping obtained by solving eqns (26a) and (28) with respect to λ, Θ_1 and Θ_2 is equal to $\tilde{\lambda}_D = 0.248432$ that is 1.2% smaller than λ_D which

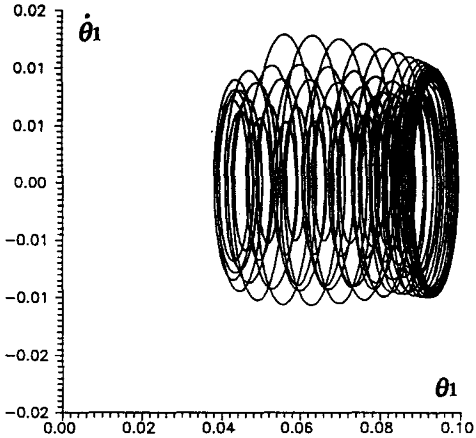

a)Stable motion (λ=0.343737 < λ_{DD})

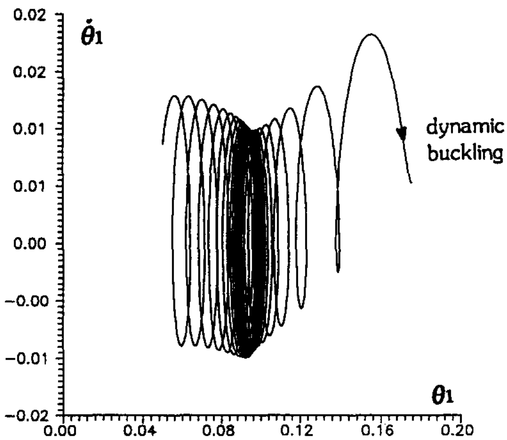

b)Dynamic buckling (λ=0.343750 > λ_{DD})

Fig. 9. Phase plane portraits for the case of impact loading with $\delta_1 = -2.5$, $\delta_2 = -0.75$, $\varepsilon_1 = 0.05$, $\varepsilon_2 = -0.031$, $\bar{c}_1 = 0.001$, $\bar{c}_2 = 0.001$, $\mu_1 = 1.84$, $\mu_0 = 0.08$, $\bar{v}_0 = 4$.

corresponds to the undamped model. Note that corresponding to this case $K^0 = 0.0001117$ and $V_T\ (\Theta_1^s, \Theta_2^s, \lambda_s) = -0.0003256$ satisfy inequality (27). In Figs 6(a,b) and 7(a,b) one can see the phase-plane portraits before (for $\lambda < \lambda_{DD}$) and after dynamic buckling (for $\lambda > \lambda_{DD}$) for the case of a step loading of infinite duration ($\bar{v}_0 = 0$) and of impact loading ($\bar{v}_0 = 4$), respectively.

If $\varepsilon_2 = 0$ is replaced by $\varepsilon_2 = -0.031$ and $\mu_1 = 1.84$, while the values of the other parameters remain constant the model under statically applied load loses its stability via a limit point with corresponding load $\lambda_s = 0.360813$. In case of a step load of infinite duration ($\bar{v}_0 = 0$) dynamic buckling occurs at $\lambda_D = 0.355003$ (undamped model) and at $\lambda_{DD} = 0.3552479$ for a damped model with $\bar{c}_1 = \bar{c}_2 = 0.001$. For vanishing (but non-zero) damping we find $\tilde{\lambda}_D = 0.328236$. The same model under impact load with $\bar{v}_0 = 4$ and $\mu_0 = 0.08$ buckles dynamically at $\lambda_D = 0.343630$ (undamped model) and at $\lambda_{DD} = 0.343738$ for a damped model with $\bar{c}_1 = \bar{c}_2 = 0.001$. For vanishing (but nonzero) damping we obtain $\tilde{\lambda}_D = 0.312893$, i.e. 9.8% smaller than λ_D. In this case $K^0 = 0.0002305$, while $U_T(\Theta_1^s, \Theta_2^s, \lambda_s) = -0.00010 < K^0$. In Figs 8(a,b) and 9(a,b) one can see the phase-plane portraits before and after dynamic buckling for the case of a loading of infinite duration ($\bar{v}_0 = 0$) and of impact loading ($\bar{v}_0 = 4$), respectively.

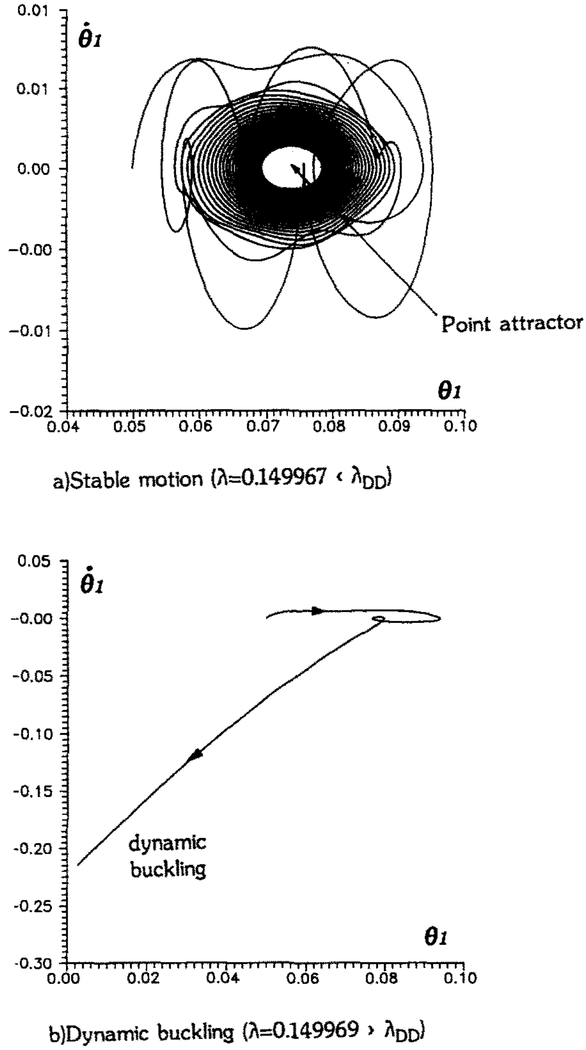

Fig. 10. Phase plane portraits for the case of step loading of infinite duration with $\delta_1 = 1$, $\delta_2 = -10.1$, $\varepsilon_1 = 0.05$, $\varepsilon_2 = 0.05$, $\bar{c}_1 = 0.02$, $\bar{c}_2 = 0.04$, $\mu_1 = 1.84$, $\bar{v}_0 = 0$.

For a geometrically imperfect system, $\varepsilon_1 = \varepsilon_2 = \varepsilon = 0.05$ and $\mu_1 = 1.84$ for which $\delta_1 = 1$ and $\delta_2 = -10.1$, we find that the loss of static stability takes place through a limit point at $\lambda_s = 0.1858309 < \lambda_c = 0.5\,(3-\sqrt{5}) = 0.381966$, where λ_c is the bifurcational load. The initial kinetic energy K^0 due to the initial conditions (22) for the case of impact load for $\dot{\Theta}_1(0) \neq 0$ is

$$K^0 = \frac{1}{2}\frac{\mu_0^2 \bar{v}_0^2}{\mu_1}\sin^2 \varepsilon \tag{36}$$

while for $\dot{\Theta}_1(0) = 0$ it becomes

$$K^0 = \tfrac{1}{2}\mu_0^2 \bar{v}_0^2 \sin^2 \varepsilon. \tag{37}$$

Between the last two values of K^0 we must take into account that value which yields the minimum buckling load. For the values $\mu_1 = 1.84$, $\mu_0 = 0.08$, $\bar{v}_0 = 4$, $\varepsilon_1 = \varepsilon_2 = 0.05$, $\bar{c}_1 = 0.02$ and $\bar{c}_2 = 0.04$ eqns (20) yield $\lambda_D = 0.140241$ and $\lambda_{DD} = 0.143503$. For vanishing damping (i.e. $c_1 = c_2 \to 0$) we obtain $\tilde{\lambda}_D = 0.136343$. If $\bar{v}_0 = 0$ (step load of infinite duration) and $\bar{c}_1 = 0.02$ and $\bar{c}_2 = 0.04$ we obtain $\lambda_{DD} = 0.149968$, while for $c_1 = c_2 = 0$ we find

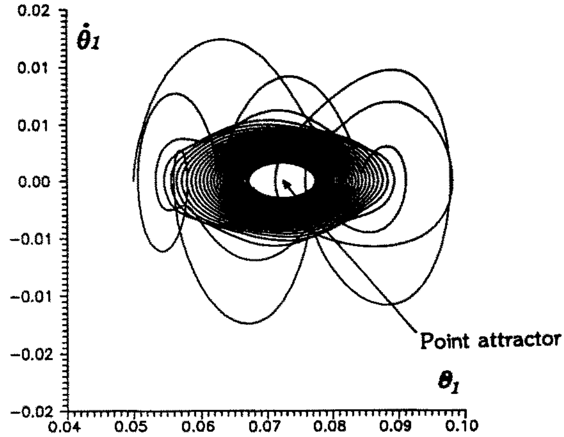

a)Stable motion (λ=0.143502 < λ_{DD})

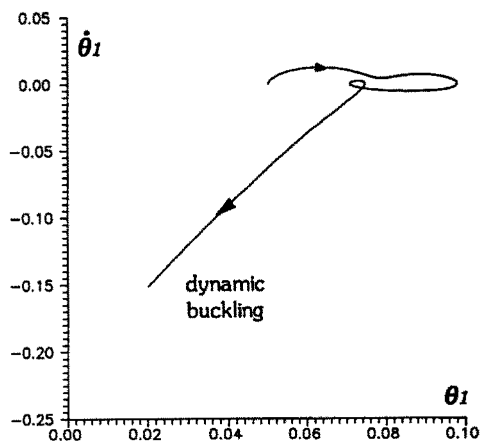

b)Dynamic buckling (λ=0.143504 > λ_{DD})

Fig. 11. Phase plane portraits for the case of impact loading with $\delta_1 = 1$, $\delta_2 = -10.1$, $\varepsilon_1 = 0.05$, $\varepsilon_2 = 0.05$, $\bar{c}_1 = 0.02$, $\bar{c}_2 = 0.04$, $\mu_1 = 1.84$, $\mu_0 = 0.08$, $\bar{v}_0 = 4$.

$\lambda_D = 0.147979$. For vanishing damping it follows that $\tilde{\lambda}_D \doteq 0.1469358$. Finally, Figs 10(a,b) and 11(a,b) show the phase-plane portraits before and after dynamic buckling for the above cases $\bar{v}_0 = 4$ (impact load), and $\bar{v}_0 = 0$ (step load of infinite duration).

REFERENCES

Goldsmith, W. (1960). *IMPACT, the Theory and Physical Behavior of Colliding Solids*. Edward Arnold, London.

Kounadis, A. N. (1991a). Nonlinear dynamic buckling of discrete dissipative or non-dissipative systems under step loading. *AIAA Jl* **29**(3), 280–289.

Kounadis, A. N. (1991b). Chaoslike phenomena in the nonlinear dynamic stability of discrete damped or undamped systems under step loading. *Int. J. Non-lin. Mech.* **26**(3/4), 301–311.

Kounadis, A. N. (1993). Static and dynamic, local and global, bifurcations in nonlinear autonomous structural systems. *AIAA Jl* (to be published).

Kalathas, N. and Kounadis, A. N. (1991). Metastability and chaoslike phenomena in nonlinear dynamic buckling of a simple two-mass system under step load. *Arch. Appl. Mech.* **61**, 162–179.

Kounadis, A. N., Mahrenholtz, O. and Bogacz, R. (1990). Non-linear dynamic stability of a simple floating bridge model. *Ing-Arch.* **60**, 262–273.

Kounadis, A. N. and Raftoyiannis, J. (1990). Dynamic stability criteria of nonlinear elastic damped/undamped systems under step loading, *AIAA Jl* **28**(7), 1217–1223.

Raftoyiannis, J. and Kounadis, A. N. (1988). Dynamic buckling of limit point systems under step loading. *Dynam. Stability Syst.* **3**(3/4), 219–234.